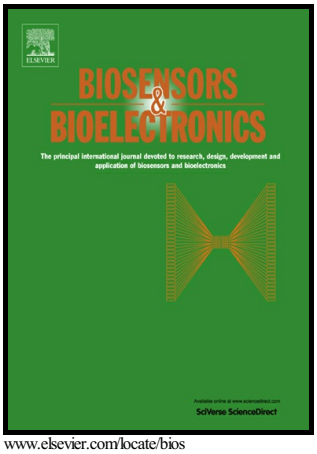

www.elsevier.com/locate/bios

Direct growth of metal-organic frameworks thin film arrays on glassy carbon electrode based on rapid conversion step mediated by copper clusters and hydroxide nanotubes for fabrication of a high performance non-enzymatic glucose sensing platform

Saeed Shahrokhian, Elnaz Khaki-Sanati, Hadi Hosseini

PII: S0956-5663(18)30299-9
DOI: https://doi.org/10.1016/j.bios.2018.04.039
Reference: BIOS10435

To appear in: *Biosensors and Bioelectronic*

Received date: 11 February 2018
Revised date: 1 April 2018
Accepted date: 17 April 2018

Cite this article as: Saeed Shahrokhian, Elnaz Khaki-Sanati and Hadi Hosseini, Direct growth of metal-organic frameworks thin film arrays on glassy carbon electrode based on rapid conversion step mediated by copper clusters and hydroxide nanotubes for fabrication of a high performance non-enzymatic glucose sensing platform, *Biosensors and Bioelectronic,* https://doi.org/10.1016/j.bios.2018.04.039

Direct growth of metal-organic frameworks thin film arrays on glassy carbon electrode based on rapid conversion step mediated by copper clusters and hydroxide nanotubes for fabrication of a high performance non-enzymatic glucose sensing platform

Saeed Shahrokhian[a,b*], Elnaz Khaki-Sanati[a], Hadi Hosseini[a]

[a]Department of Chemistry, Sharif University of Technology, Tehran 11155–9516, Iran

[b]Institute for Nanoscience and Technology, Sharif University of Technology, Tehran, Iran

[*]Corresponding author: shahrokhian@sharif.edu

Abstract. The direct growth of self-supported metal-organic frameworks (MOFs) thin film can be considered as an effective strategy for fabrication of the advanced modified electrodes in sensors and biosensor applications. However, most of the fabricated MOFs-based sensors suffer from some drawbacks such as time consuming for synthesis of MOF and electrode making, need of a binder or an additive layer, need of expensive equipment and use of hazardous solvents. Here, a novel free-standing MOFs-based modified electrode was fabricated by the rapid direct growth of MOFs on the surface of the glassy carbon electrode (GCE). In this method, direct growth of MOFs was occurred by the formation of vertically aligned arrays of Cu clusters and $Cu(OH)_2$ nanotubes, which can act as both mediator and positioning fixing factor for the rapid formation of self-supported MOFs on GCE surface. The effect of both chemically and electrochemically formed $Cu(OH)_2$ nanotubes on the morphological and electrochemical performance of the prepared MOFs were investigated. Due to the unique properties of the prepared MOFs thin film electrode such as uniform and vertically aligned structure, excellent stability, high electroactive surface area, and good availability to analyte and electrolyte diffusion, it was directly used as the electrode material for non-enzymatic electrocatalytic oxidation of glucose. Moreover, the potential utility of this sensing platform for the analytical determination of glucose concentration was evaluated by the amperometry technique. The results proved that the self-supported MOFs thin film on GCE is a promising electrode material for fabricating and designing non-enzymatic glucose sensors.

Keywords: Direct growth, MOFs thin film; Amperometry; Non-enzymatic glucose sensor; Glassy carbon electrode; Surface modification

1. Introduction

One of the most important subjects in material science, chemistry, and biotechnology is the surface modification of solid substrate (Kang et al., 2012; Lane et al., 2017). The modification mostly includes the control of surface properties by addition of a coating, a second material that can be synthesized in diverse methods, according to the coating material and substrate nature and features. These techniques can be widely used in various fields include nanotechnological and electrical devices, catalytic and electrocatalytic, sensing and bio-sensing, and multitude other advanced devices (Kang et al., 2012; Lane et al., 2017;). One of the most remarkable class of materials for coating applications are micro and nano porous materials (Silva et al., 2015). Metal organic framework (MOF) materials are the spotlight of porous materials in extensive research domains, especially in chemical industry and material science in last three decades, owing to their wonderful nature and surprising characteristics (Rowsell and Yaghi 2004; Silva et al., 2015; Stock and Biswas 2011). MOF compounds are self-assembly polymerized by interconnection of metal (or metal oxide clusters) with rigid organic ligands (as linkers) to construct infinite hollow structures (Rowsell and Yaghi 2004; Silva et al., 2015; Stock and Biswas 2011).

The ability for wide range selections of metals and linkers in MOFs preparation can make adjustable structures with tunable nanopores, which induce unique properties such as ultra-high interfacial, accessible metal sites, open framework structure and adjustable functionalities in the obtained structures (Rowsell and Yaghi 2004; Silva et al., 2015; Stock and Biswas 2011). Moreover, such unique properties can make these materials as promising candidates for application in different tasks like catalysis and electrocatalysis (Aguirre et al., 2015; Furukawa et al., 2013; Hosseini et al., 2013), sensing (Hosseini et al., 2013; Liu et al., 2011), separation (Li et al., 2012), and storage (Bae and Snurr 2011; Banerjee et al., 2015). In the other words, in order

to utilize the noteworthy features of these ultra-porous crystals in advanced systems like electric and nanotechnological devices, MOF materials must be positioned in the accurate location as coating or thin film on a device (Coclite et al., 2013; Li et al., 2016; Stavila et al., 2014; Talin et al., 2014). In this regard, various strategies for deposition of MOF thin continuous films have been developed like solvothermal (Rodenas et al., 2015), microwave-induced (Yooa and Jeong 2008), self-assembled monolayer (Biemmi et al., 2007), evaporation-induced (Ameloot et al., 2010), gel layer synthesis (Schoedel et al., 2010), liquid phase epitaxy (Shekhah et al., 2009), layer by layer deposition (Makiura et al., 2010), electrochemical deposition (Campagnol et al., 2016), seeded growth (Falcaro et al., 2011), and in-situ growth methods (Guo et al., 2009; Liu et al., 2011; Okada et al., 2014; Qi et al., 2014). Among all these methods, in-situ growth is a powerful and straightforward method that includes only a couple of facile conversion steps. In this method, MOF thin film can be directly grown on the substrate without any requirement to binders for immobilization of active materials or additives like an organic layer, which all are barriers through electrical conductivity and accessibility to active surface area. Moreover, the direct growth of MOFs films without using an organic layer has been scarcely reported (Guo et al., 2009; Liu et al., 2011; Okada et al., 2014; Qi et al., 2014). In this regard, an efficient method for controlling the MOF growth can be done by producing an intermediate, which afterwards converted to MOF by a chemical reaction. For example, Falaro et al. were recently presented the in-situ growth of the HKUST-1 ($Cu_3(BTC)_2$, H_3BTC: 1,3,5-benzenetricarboxylic acid) on a metallic copper substrate for the first time, which included two sequential chemical reaction steps (Okada et al., 2014). The first step is oxidation of metallic copper to copper hydroxide and the second step is conversion of copper hydroxide to HKUST-1. The reaction process is extraordinary fast and complete in 30 min. Moreover, the fabricated free-standing electrode was

used to fabricate a printed circuit board (PCB) because the most printed circuit board utilizes copper based conductive circuits (Okada et al., 2014). This direct growth strategy has revealed exclusive properties that can justify its capabilities for application in the various fields. One of the important applications of this strategy can be proposed by applying for surface modification in electrochemical sensor fabrication, due to the necessity of accurate, easy and quick detection platforms for trace determination of biological compounds and other important elements. However, utilization and improvement of this method for the surface modification of the conventional electrodes like glassy carbon electrode (GCE) as a carbon based electrode for sensing application has not been reported yet. In addition, the use of GCE is very common and well-known in electrochemical sensing platforms because it has a controllable surface area, wide potential window, excellent mechanical and chemical stability in various medium as compared to copper foil. It is also noteworthy that due to the slow electron transfer of many vital analytes, their detection is hindered at the GCE surface. Therefore, the electrode surface modification is essential for improving the sensitivity of the electrochemical determinations (Kimmel et al., 2012; Zhu et al., 2015). In the field of electrochemical sensing, most of the MOF modified GCE electrodes were fabricated by some conventional methods that suffer from some drawbacks, such as time consuming of both MOF synthesis and electrode fabrication, need to a binder or an additive layer, rough conditions like high pressure and temperature, need of sophisticated equipment and use of hazardous solvents (Lie et al., 2014). Thus, there is a requirement to represent more efficient, simpler and faster modification procedures in order to deposit a uniform, compact and well-adherent layer of MOF crystals on GCE surface, which can lead to obtaining a high performance electrochemical sensing platform.

In the recent years, accurate non-enzymatic sensing of glucose has a great technological and scientific importance for clinical diagnosis of diabetes and other analytical applications in food and pharmaceutical industries, biotechnology and control of environmental pollution (Wang 2008; Asadian et al., 2016; Asadian et al., 2018). Among various electrode materials, copper-based materials can be considered as an excellent electrocatalyst candidate for fabrication of non-enzymatic glucose sensors owning to their advantages of low cost, high electrical conductivity, and chloride poisoning resistance (Niu et al., 2014; Zhang et al., 2012). Moreover, copper-based MOFs are a notable class of copper-based materials that can be used as an electrocatalyst due to their unique properties such as ultra-high porosity and electrocatalytic activity, which can lead to the efficient amplification of the voltammetric signals (Hosseini et al., 2013; Hosseini et al., 2013; Lei et al., 2014). However, as it mentioned, because of aforementioned challenges for direct growth of MOFs thin layers on the GCE surface, more investigations have to be done to serve the purpose of the surface modification method with fast, simple, reliable, efficient and low cost properties.

Herein, we have developed a novel non-enzymatic glucose sensing platform based on the surface modification of GCE by the in-situ direct growth of MOF thin film for the first time, which contains literally fast and highly controllable two conversion steps. This method shows how we can elaborate design a free-standing MOF thin film on the GCE surface based on the controllable conversion of the prepared copper hydroxide nanotubes ($Cu(OH)_2$ NTs), as a conversion mediator, to MOF thin film. Total conversions procedure needs only 4 min to be completed. In this process, at first, well-adherent Cu clusters that consist of copper nanoparticles were vertically electrodeposited on the GCE from sulfate solution by applying a constant reductive voltage, which their unique orientations can lead to the high surface area and better

availability of the surface to form $Cu(OH)_2$ NT structures, as compared to the commercial copper foil (Okada et al., 2014). Then, the uniform and compact layer of scroll-type nanotube structure of $Cu(OH)_2$ was successfully fabricated on copper clusters substrate by both chemical and electrochemical approach at ambient conditions. Finally, an ultra-fast conversion of $Cu(OH)_2$ precursor into free-standing MOFs was occurred in ethanoic aqueous linker solution at the room temperature without need of any hazardous solvents like DMF (N,N-dimethylformamide). In comparison to former reported methods, the present method shows great ecological and economical advantages. The electrochemical performance of the free-standing MOF electrode, prepared from both chemically and electrochemically formed $Cu(OH)_2$ NTs, was fully evaluated in electrocatalytic oxidation and ultra-trace determination of glucose.

2. Experimental

The $Cu(OH)_2$ NTs are prepared both chemically and electrochemically on GCE and their resulted MOFs were named c-MOFs@GCE and e-MOFs@GCE, respectively. Experimental details for the electrode fabrication and analytical assessments are available in the Supporting Information.

3. Result and Discussion

3.1. Materials Characterization

The procedure for preparation of $Cu(OH)_2$ nanotubes (NTs) from the electrodeposited copper on GCE and their conversion to c-MOFs coatings is depicted in Fig. 1 A. The protocol can be summarized as a three step approach; the electrodeposition of metallic copper on the surface of GCE (Cu@GCE), the conversion of Cu@GCE to $Cu(OH)_2$ NTs@GCE, and the

conversion of $Cu(OH)_2$ NTs@GCE to MOFs@GCE. At first, the morphology of the deposited metallic copper on the surface of GCE was analyzed using FE-SEM. Under the optimum potential (-0.25 V) and deposition time (400 s), a well-ordered cluster arrays of Cu were uniformly and vertically deposited on the surface of GCE, which is made up by accumulation of small Cu particles (Fig. 1 B, b dotted circles and Fig. 1S). These orientations can lead to the better availability of the surface to form $Cu(OH)_2$ NT structures as compared to the commercial copper foil.

The conversion of the obtained copper clusters to coper hydroxide NTs were carried out by the following oxidation procedure stablished by Zhang et al. (Zhang et al., 2003) who proposed how to design single crystal NT arrays of $Cu(OH)_2$:

$$Cu + 4NaOH + (NH_4)_2S_2O_8 \rightarrow Cu(OH)_2 + 2Na_2SO_4 + 2NH_3 \uparrow + 2H_2O \qquad (1)$$

In this process, the formation of $Cu(OH)_2$ NTs@GCE was carried out by immersion of Cu@GCE into an aqueous solution of $(NH_4)_2S_2O_8$ and NaOH, as described in the experimental section. After 4 min of the reaction, the transformation of Cu@GCE to $Cu(OH)_2$ NTs@GCE was almost completed and the conversion was detected using FE-SEM (Fig. 1 C). The low-magnification FE-SEM image reveals that the uniform and compact structure of $Cu(OH)_2$ with a scroll-like morphology is obtained on the whole surface of GCE by simple immersion in the alkaline-oxidative solution (Fig. 1 C). However, the high magnification of $Cu(OH)_2$ NTs revealed that a tubular structure of wires with the length of 3 micrometers and the diameter of 100 nm is formed (Fig. 1 C(d)). Furthermore, the $Cu(OH)_2$ NTs have grown in different directions that may be related to the cluster nature of the electrodeposited Cu metal on the

surface of GCE. Thus, more $Cu(OH)_2$ NTs can be formed as compared to commercial copper foil (Okada et al., 2014; Zhang et al., 2003). In addition, the results showed that the formation of $Cu(OH)_2$ NTs on the surface of GCE (4 min) is much faster than the formation on commercial copper foil (Okada et al., 2014; Zhang et al., 2003), which confirmed the convenience and low time taken for the electrode modification, which is a critical factor in analytical applications.

After the formation of $Cu(OH)_2$ NTs, the final step is the formation of c-MOFs@GCE that requires the immersion of the $Cu(OH)_2$ NTs@GCE into a mixture of alcohol, water, and trimesic acid (H_3BTC), as described in the experimental section. During this process, the conversion from the copper hydroxide into a Cu-based MOF was performed only after a few minutes at room temperature (Figs. 1A and 2). Most of the synthesis method of MOFs usually suffer from time consuming processes such as hydrothermal and reflux methods, which also used hazardous solvent and soluble metal salts such as nitrates that are appears as oxidizers and may constitute a safety hazard in the industrial applications. However, the conversion of $Cu(OH)_2$ NTs into c-MOFs would be desirable and the related chemical mechanism can be expressed as a simple acid-base reaction:

$$3Cu(OH)_2 + 2H_3BTC \rightarrow Cu_3(BTC)_2 + 6H_2O \qquad (2)$$

Which is waste-free, safe, and fast reaction without the use of hazardous solvents and metal salts (Majano and Pérez-Ramírez 2013).

Moreover, the homogeneous and uniform formation of well-aligned $Cu(OH)_2$ NTs on the surface of GCE provides the appropriate conditions for the rapid formation of c-MOFs. The FE-SEM images of the formed c-MOFs@GCE with a low magnification confirm the rapid, and efficient direct growth of MOFs crystals on the surface of GCE using $Cu(OH)_2$ NTs (Fig. 2) only after 4 min. In addition, the uniform MOFs crystals are formed on the surface of GCE as compared to copper foil (Fig. 2S), which is desirable for sensing applications.

The high-magnification FE-SEM images confirmed that the growth c-MOFs octahedral crystals have a particle size between 0.5 and 1.2 μm. The $Cu(OH)_2$ NTs immersed in the BTC ligand after only 30 second reaction time more proved that the transformation is very fast, because most of the $Cu(OH)_2$ NTs are converted to the octahedral c-MOFs particles with a smaller size as compared to 4 min reaction time and confirmed the direct instantaneous formation of MOFs (Fig. 3 A). Furthermore, the Fig. 3 A(b) clearly shows the role of NTs in the construction of octahedral c-MOFs (Dashed circles). In fact, it seems that the NTs are gathered together in the presence of BTC ligands, which leads to the fabrication of octahedral c-MOFs structures. Moreover, due to the fast, easy, and one-way irreversible chemical reaction of eq. 1, the $Cu(OH)_2$ NTs can be easily rearrangement into c-MOFs octahedral structures in the presence of BTC ligand. Consequently, the prepared well-separated and defined octahedral c-MOFs on GCE with an excellent stability, precisely controlled morphology and high surface area can be directly used as a sensing platform in the electrochemical detections without using any insulating binder or conductive additives that cause to increased resistivity and dead weight of the electrode, respectively. This structure can offer shorten diffusion path length for the analyte species and the

electrolyte ions in the porous crystalline structure and easy accessibility to the electroactive sites in the self-standing MOFs, which can lead to a high performance sensing platform.

The EDX spectra confirm the presence of C, O, and Cu elements within the formed c-MOFs (Fig. 2). Furthermore, the EDX mapping shows the uniform distribution of these elements on the whole surface of GCE (Fig. 3S), which is in agreement with the FE-SEM results. For further studies, the $Cu(OH)_2$ structures were synthesized using the electrochemical approach by anodizing of Cu@GCE at a constant current of 0.2 mA during 180 s in the 3.0 M NaOH solution. Similar to the chemically formed $Cu(OH)_2$ NTs, the FE-SEM images show the tubular structure of the formed $Cu(OH)_2$ with different orientations due to the cluster nature of the deposited Cu on the surface of GCE (Fig. 3 B). In addition, Fig. 4S clearly showed the effect of Cu clusters in the orientation of generated $Cu(OH)_2$ NTs. Similarly, the FE-SEM images of the prepared e-MOFs@GCE confirm the successful conversion of the electrochemically prepared $Cu(OH)_2$ NTs to the MOFs (Fig. 5S). Moreover, the prepared $Cu(OH)_2$ NTs using both chemically and electrochemically approaches, and resulting MOFs show little differences in morphology in the terms of diameter, crystal shape and size, which may lead to differences in their electrochemical performances and kinetics of the electron transfer processes. The XRD and FT-IR investigations were shown in the supporting information (Fig. 6S).

Generally, the materials characterizations showed that the residual $Cu(OH)_2$ can be observed in FE-SEM, XRD (Fig. 6S A) and FT-IR (Fig. 6S B) investigations that might play an important role for the adhesion properties and stability of the prepared MOFs, because it can act as a conductive binder or conversion layer between the substrate and the MOFs.

3.2. Electrochemical characterizations

3.2.1. Cyclic voltammetric studies

The prepared self-supported MOFs on GCE surface can be guaranteed the full accessibility of the electroactive sites in the MOFs microcubes to the analyte species in the electrochemical sensing, yielding a high signal-to-noise ratio (S/N) and excellent electrochemical responses. Thus, in order to characterize the electrochemical performances of the prepared MOFs modified electrodes in electrochemical sensing applications, the electrocatalytic ability of $Cu(OH)_2$ NTs@GCE and c-MOFs@GCE were evaluated using cyclic voltammetry (CV) toward the glucose oxidation. Fig. 4 (A to D) shows the CVs responses of $Cu(OH)_2$ NTs@GCE and c-MOFs@GCE in the absence (a) and the presence of 0.27 mM glucose (b) in 0.1 M NaOH within the potential window from -0.6 V to +0.5 V at a scan rate of 10 mV/s. As can be seen, the bare GCE does not display any electrochemical activity toward the glucose oxidation over the applied potential range. In addition, only a minor background current was obtained and no response to glucose was observed on the surface of GCE (Fig. 4 A). In the absence of glucose, the $Cu(OH)_2$ NTs@GCE shows a well-defined anodic peak at -0.12 V related to the transition of Cu(0) to Cu(II) hydroxide and a broad oxidation peak between 0.0 to 0.5 V related to the transition of Cu(I) to Cu(II) and Cu(II) to Cu(III) hydroxide forms in the positive direction, while a strong cathodic peak at -0.44 V was appeared in the negative direction, which can be related to the transition of Cu(II)/Cu(I) (Mariolia and Kuwanab 1992; Li et al., 2015; Luo et al., 1990; Luo and Baldwin 1995; Zhang et al., 2012; Zhang et al., 2012). The obtained CVs show some differences in the presence of glucose and a new irreversible anodic peak starts to appear at about +0.4 V on the surface of $Cu(OH)_2$ NTs@GCE that can be imputed to the oxidation of glucose. In the case of c-MOFs@GCE, an analogous electrochemical change was observed for the oxidation

of glucose. However, the enhancement of catalytic current of c-MOFs@GCE related to the oxidation of glucose is greater than that of $Cu(OH)_2$ NTs@GCE, which confirm that the MOFs have superior electrocatalytic activity and larger active surface area as compared to $Cu(OH)_2$ NTs@GCE. Thus, the c-MOFs@GCE could be considered as an effective electrocatalyst for oxidation and sensing of glucose.

Although the precise mechanism for the electro-oxidation of glucose on copper-based modified electrodes in alkaline electrolyte was not still known with assurance, the most confirmed one is that represented by Mariolia and Kuwanab (Mariolia and Kuwanab 1992). They proposed that the oxidation was activated by the deprotonation of glucose and isomerization to its enediol form at the surface of the electrode and oxidation by Cu(I), Cu(II) and Cu(III). Among various valence states of Cu hydroxides, the Cu(III) species, such as CuOOH, plays a main role in the glucose oxidation. In the other hand, when the potential is between 0.30 V to 0.50 V the oxidation peak of glucose was appeared because it would be catalyzed tremendously due to the formation of Cu (III) species as a main electron transfer mediator in this range (Mariolia and Kuwanab 1992; Li et al., 2015; Luo et al., 1990; Luo and Baldwin 1995; Zhang et al., 2012). Furthermore, when glucose was added to the alkaline solution, the anodic peak was decreased due to the formation of Cu(I)–glucose complex at the potential of -0.12 V. The cathodic peak current, corresponding to the conversion of Cu(II)/Cu(I), shows a tiny diminishing due to interaction between glucose and Cu(I) species (Mariolia and Kuwanab 1992; Li et al., 2015; Luo et al., 1990; Luo and Baldwin 1995; Zhang et al., 2012). The whole process for the electro-oxidation of glucose on the surface of the prepared copper based electrodes can be summarized as follow:

$$Cu(OH)_2 + OH^- \leftrightarrow CuOOH + H_2O + e^- \quad (3)$$

$$CuOOH + Glucose + e^- \rightarrow CuO + OH^- + \text{Gluconolactone} \quad (4)$$

$$\text{Gluconolactone} \xrightarrow{Hydrolysis} \text{Gluconic acid} \quad (5)$$

$$CuO + OH^- \leftrightarrow CuOOH + e^- \quad (6)$$

The correlation between the catalytic peak current and glucose concentration was also studied (Fig. 4 E and F). By increasing the glucose concentration (a to g) in the alkaline medium, more and more Cu(III) species at c-MOFs@GCE modified electrode would be involved in the electrochemical reaction Fig. 4 E, resulting in the enhancement of glucose electro-oxidation peak current and diminution of anodic peak current due to the formation of Cu(I)–glucose complex. These results confirmed that the c-MOFs@GCE can effectively respond to the changing glucose concentration. Also, the current response remained approximately unchanged after consecutive scanning, which demonstrates the high stability of the c-MOFs@GCE toward the oxidation of glucose in alkaline medium and confirm the capacity of c-MOFs@GCE for fabrication as an effective glucose sensor. For more comparison, the electrochemical performance of e-MOFs@GCE was also investigated using CV (Fig. 4 F). Its behavior was approximately similar to c-MOFs@GCE. The difference is that the enhancement of catalytic current by addition of specific amounts of glucose on the mentioned electrode is partially more than that of c-MOF@GCE, which may be related to the higher surface area of this MOF. In addition, the e-MOFs@GCE shows a well-defined anodic peak between 0.3 to 0.5 V in the absence of glucose, indicating formation of higher amounts of Cu(III) hydroxide or oxide as the main electron transfer mediators at the electrode surface, which further confirms the enhancement of the catalytic oxidation of glucose on the surface of this MOF-based electrode.

Moreover, the electrochemical oxidation of glucose on the surface of c-MOFs@GCE was studied in the phosphate buffer solution of pH 8.0 (Fig. 7S). No considerable electrocatalytic activity was observed for the glucose oxidation on the surface of c-MOFs@GCE in the phosphate buffer solution as compared to the NaOH solution. Thus, it can be more confirmed that Cu(II)/Cu(III) is the main electron transfer agent in the glucose oxidation because the conversion of Cu(II)/Cu(III) must be taken place by incorporation of OH^- ion and the NaOH electrolyte is required to carry out this transition (Eq. 3). In addition, the stability of our electrode in the NaOH electrolyte is much better than the phosphate buffer solution. Therefore, the NaOH was chosen as the supporting electrolyte to create electrocatalytic active sites for the glucose oxidation and its sensing.

3.2.2. Chronoamperometric studies

In order to determine the electrochemical kinetic and electrocatalytic parameters of c-MOFs@GCE toward the glucose oxidation, further investigations were carried out by chronoamperometry technique. Fig. 5 shows the chronoamperometric responses of (A) $Cu(OH)_2$ NTs@GCE, and (B) c-MOFs@GCE in different concentrations of glucose (a to d: from 0 to 0.3 mM) in 0.1 M NaOH at a constant potential of 0.5 V (vs. Ag/AgCl). In comparison with $Cu(OH)_2$ NTs@GCE, the c-MOFs@GCE render higher steady state currents at each specific concentration of glucose, which is in agreement with the CV data. Furthermore, the relative surface area ratio between $Cu(OH)_2$ NTs@GCE and c-MOFs@GCE was estimated using

chronoamperometry and Cottrell equation (Bard and Faulkner 2001; Galus and Harwood 1976). According to the Cottrell equation, the variation of current by elapsed time in diffusion-controlled processes can be described by the following:

$$I = nFAD^{1/2}C\pi^{-1/2}t^{-1/2} \qquad (7)$$

Where n is the number of the transferred electrons, F is the Faraday constant, A is the surface area of electrode (cm^2), D is the glucose diffusion coefficient ($cm^2. s^{-1}$) and C is the bulk glucose concentration ($mol.cm^{-3}$). Because the number of electron transferred is similar for both $Cu(OH)_2$ NTs@GCE and c-MOFs@GCE, as copper-based electrodes, the relative surface area ratio can be obtained from the plot of the oxidation current vs. the inversed square root of the passed time using Eq. 7 (Fig. 5 C). The slope of the lines demonstrates that the surface area of c-MOFs@GCE is about 2.6 times greater than $Cu(OH)_2$ NTs@GCE, which revealed the fact that formation of MOF nanostructure creates a considerably larger active surface area. For calculating the catalytic rate constant, still chronoamperometric technique was applied. At the middle of time points, when the current was confined by the rate of the electrocatalytic oxidation of glucose, the catalytic current could be display in following equation:

$$\frac{I_{cat}}{I_L} = (\pi k_{cat} C_0 t)^{1/2} \qquad (8)$$

Where I_{cat} and I_L are the oxidation currents of the c-MOFs@GCE in the presence and absence of glucose, respectively. C_0 is the bulk glucose concentration (M), t is the time elapsed. According to the equation (8), k_{cat} can be calculated from the slope of I_{cat}/I_L vs. $t^{1/2}$ plot. The average value

of calculated k_{cat} was 9.5×10^4 M^{-1} s^{-1} (or 9.5×10^4 cm^3 mol^{-1} s^{-1}), suggesting the high rate capability of prepared MOF for oxidation of glucose as compared to the reported value for copper based electrodes (Table 1S), which can lead to the fast response of the sensor in the analytical applications.

3.2.3. Amperometric studies for the glucose detection

As discussed above, the prepared MOFs modified GCEs show considerable electrocatalytic activities towards the glucose oxidation. Therefore, they can act as effective electrochemical sensing platforms for the non-enzymatic detection of glucose. To achieve this goal, the amperometry technique was applied. The results about the amperometric detection of glucose, and also repeatability, reproducibility and selectivity of the prepared electrodes, and real sample analysis were available in the supporting information.

4. Conclusions

In this work, we used a simple and facile protocol for preparation of self-supported MOFs on GCE. In addition, the protocol is environmentally friendly, low cost, and rapid as compared to other direct MOF growth techniques such as electrochemical, and even in-situ growth methods, because it only used ethanol as an organic solvent and requires only 4 min to form when the substrate is ready for the conversion. The rapid growth of the MOFs on GCE can be ascribed to the clustery formation of the copper film on GCE that has excellent surface availability to form highly uniform and well-defined $Cu(OH)_2$ nanotubes which act as an intermediate and

positioning fixing factor in the rapid formation of self-supported MOFs on GCE. A novel non-enzymatic glucose sensor has been developed based on the electrocatalytic properties of the self-supported MOFs on GCE, which exhibits excellent electrocatalytic ability toward glucose oxidation in aqueous NaOH solution. This sensing platform can provide a strong proof for the study of this kind of self-supported MOFs for construction of attractive sensor in the future.

Acknowledgements

The authors gratefully acknowledge the financial support of this work by the Research Council (Grant No. G930616). They also acknowledge the Center of Excellence for Nanostructures of the Sharif University of Technology, Tehran, Iran.

References

Aguirre-Díaz, L.M., Gándara, F., Iglesias, M., Snejko, N., Gutiérrez-Puebla, E., Monge, M. Á., 2015. J. Am. Chem. Soc. 137, 6132-6135.

Ameloot, R., Gobechiya, E., Uji-I, H., Martens, J.A., Hofkens, J., Alaerts, L., Sels, B.F., De Vos, D.E., 2010. Adv. Mater. 22, 2685-2688.

Asadian, E., Shahrokhian, S., Iraji Zad, A., 2016. RSC Adv. 6, 61190-61199.

Asadian, E., Shahrokhian, S., Iraji Zad, A., 2018. J. Electroanal. Chem. 808, 114-123.

Bae, Y.S., Snurr, R.Q., 2011. Angew. Chem. Int. Ed. 50, 11586-11596.

Banerjee, D., Cairns, A.J., Liu, J., Motkuri, R.K., Nune, S.K., Fernandez, C.A., Krishna, R., Strachan, D.M., Thallapally, P.K., 2015. Acc. Chem. Res. 48, 211-219.

Bard, A.J., Faulkner, L.R., 2001. Wiley; New York p. 209 ch.5.

Biemmi, E., Scherb, C., Bein, T., 2007. Am. Chem. Soc. 129, 8054-8055.

Coclite, A.M., Howden, R.M., Borrelli, D.C., Petruczok, C.D., Yang, R., Yagüe, J.L., Ugur, A., Chen, N., Lee, S., Jo, W.J., Liu, A., Wang, X., Gleason, K.K., 2013. Adv. Mater. 25, 5392-5422.

Falcaro, P., Hill, A.J., Nairn, K.M., Jasieniak, J., Mardel, J.I., Bastow, T.J., Mayo, S.C., Gimona, M., Gomez, D., Whitfield, H.J., Riccò, R., Patelli, A., Marmiroli, B., Amenitsch, H., Colson, T., Villanova, L., Buso, D., 2011. Nat. Commun. 2, 237.

Furukawa, H., Cordova, K.E., O'Keeffe, M.O., Yaghi, O.M., 2013. Science 341, 974-986.

Galus, Z., Horwood, E., 1976.

Guo, H., Zhu, G., Hewitt, I.J., Qiu, S., 2009. J. Am. Chem. Soc. 131, 1646-1647.

Hosseini, H., Ahmar, H., Dehghani, A., Bagheri, A., Fakhari, A.R., Amini, M.M., 2013. Electrochim. Acta 88, 301-309.

Hosseini, H., Ahmar, H., Dehghani, A., Bagheri, A., Tadjarodi, A., Fakhari, A.R., 2013. Biosens. Bioelectron. 42, 426-429.

Kang, S.M., Hwang, N.S., Yeom, J., Park, S.Y., Messersmith, P.B., Choi, I.S., Langer, R., Anderson, D.G., Lee, H., 2012. Adv. Funct. Mater. 22, 2949-2955.

Kimmel, D.W., LeBlanc, G., Meschievitz, M.E., Cliffel, D.E., 2012. Anal. Chem. 84, 685–707.

Lane, A.P., Yang, X., Maher, M.J., Blachut, G., Asano, Y., Someya, Y., Mallavarapu, A., Sirard, S.M., Ellison, C.J., Willson, C.G., 2017. ACS Nano 11, 7656-7665.

Lei, L., Qian, R., Ling, P., Cui, L., Ju, H., 2014. TrAC Trend. Anal. Chem. 58, 71-78.

Li, J.R., Sculley, J., Zhou, H.C., 2012. Chem. Rev. 112, 869-932.

Li, W.J., Tu, M., Cao, R., Fischer, R.A., 2016. J. Mater. Chem. A 4, 12356-12369.

Li, Z., Chen, Y., Xin, Y., Zhang, Z., 2015. Scientific Report. 5, 16115.

Liu, J., Sun, F., Zhang, F., Wang, Z., Zhang, R., Wang, C., Qiu, S., 2011. J. Mater. Chem. 21, 3775-3778.

Luo, M.Z., Baldwin, R.P., 1995. J. Electroanal. Chem. 387, 87-94.

Luo, P., Prabhu, S.V., Baldwin, R.P., 1990. Anal. Chem. 62, 752-755.

Majano, G., Pérez- Ramírez, J., 2013. Adv. Mater. 25, 1052–1057.

Makiura, R., Motoyama, S., Umemura, Y., Yamanaka, H., Sakata, O., Kitagawa, H., 2010. Nat. Mater. 9, 565-571.

Mariolia, J.M., Kuwanab, T., 1992. Electrochim. Acta. 37, 1187-1197.

Niu, X., Li, Y., Tang, J., Hu, Y., Zhao, H., Lan, M., 2014. Biosens. Bioelectron. 51, 22-28.

Okada. K., Ricco. R., Tokudome, Y., Styles. M.J., Hill, A.J., Takahashi, M., Falcaro, P., 2014. Adv. Funct. Mater. 24, 1969-1977.

Qi, Y., Lin, S., Chen, C., Liu, Y., Qiao, Z., Kuang, X., Sua, Q., Chao, H.Y., 2014. J. Mater. Chem. A 2, 8849-8853.

Reitz, E., Jia, W., Gentile, M., Wang, Y., Lei, Y., 2008. Electroanalysis 20, 2482-2486.

Rodenas, T., Luz, I., Prieto, G., Seoane, B., Miro, H., Corma, A., Kapteijn, F., Xamena, F.X.L., Gascon, J., 2015. Nat. Mater. 14, 48-55.

Rowsell, J.L.C, Yaghi, O.M., 2004. Microporous Mesoporous Mater. 73, 3-14.

Schoedel, A., Scherb, C., Bein, T., 2010. Angew. Chem. Int. Ed. 49, 7225-7228.

Shekhah, O., Wang, H., Zacher, D., Fischer, R.A., Wöll, C., 2009. Angew. Chem., Int. Ed. 48, 5038-5041.

Silva, P., Vilela, S.M.F., Tomébc, J.P.C., Almeida Paz, F.A., 2015. Chem. Soc. Rev. 44, 6774-6803.

Stavila, V., Talin, A.A., Allendorf, M.D., 2014. Chem. Soc. Rev. 43, 5994-6010.

Stock, N., Biswas, S., 2011. Chem. Rev. 112, 933-969.

Talin, A.A., Centrone, A., Ford, A.C., Foster, M.E., Stavila, V., Haney, P., Kinney, R.A., Szalai, V., Gabaly, F.E., Yoon, H.P., Léonard, F., Allendorf, M.D., 2014. Science 343, 66-69.

Wang, J., 2008. Chem. Rev. 108, 814-825.

Yooa, Y., Jeong, H.-K., 2008. Chem. Commun. 0, 2441-2443.

Zhang, P., Zhang, L., Zhao, G., Feng, F., 2012. Microchim Acta 176, 411-417.

Zhang, Y., Su, L., Manuzzi, D., de los Monteros, H.V.E., Jia, W., Huo, D., Hou, C., Lei, Y., 2012. Biosens. Bioelectron. 31, 426-432.

Zhu, C., Yang, G., Li, H., Du, D., Lin, Y., 2015. Anal. Chem. 87, 230−249.

Fig.1. (A) The protocol for fabrication of free-standing MOFs thin films on GCE. (B) The FESEM images of electrodeposited copper on glassy carbon electrode prepared at constant potential of -0.25 V during 400 s in 0.01 M $CuSO_4$ + 0.5 M $(NH_4)_2SO_4$ solution at room temperature with different magnifications. (C) The FESEM images of scroll-like $Cu(OH)_2$ nanotubes prepared from Cu@GCE after 4 min remaining in aqueous NaOH + $(NH_4)_2S_2O_8$ solution at room temperature with different magnifications.

Fig. 2. The FESEM images of octahedral c-MOF crystals decorating the GCE surface converted from $Cu(OH)_2$ NTs@GCE after 4 min remaining in trimesic acid and alcoholic mixture in room temperature with different magnifications; EDX spectrum of prepared c-MOFs@GCE.

Fig. 3. (A) The FESEM images of $Cu(OH)_2$ NTs@GCE after 30 s remaining in trimesic acid and alcoholic mixture in room temperature. (B) The FESEM images of $Cu(OH)_2$ nanotubes formed by anodizing the Cu@GCE at constant current of 0.2 mA during 180 s in 3.0 M NaOH solution at room temperature with different magnifications.

Fig. 4. The CV curves obtained for (A) bare GCE, (B) $Cu(OH)_2$ NTs@GCE and (C) c-MOFs@GCE in the (a) absence and in the presence of (b) 0.27 mM glucose between -0.6 V to +0.6 V. (D) The comparison between different electrodes CV responses in the presence of 0.27 mM glucose in 0.1 M NaOH solution; scan rate: 10 mV/s.(E) The CV curves obtained for c-MOFs@GCE and (F) e-MOFs@GCE with consecutively increasing the glucose concentration from a (0 M) to g (0.23 mM) in 0.1 M NaOH solution; scan rate: 10 mV/s.

Fig. 5. The Chronoamperograms of (A) $Cu(OH)_2$ NTs@GCE and (B) c-MOFs@GCE in the absence (a) and presence of various glucose concentrations from (b) 0.1mM to (d) 0.3 mM in 0.1 M NaOH solution recorded at +0.5 V; (C) The plots of I_{cat} vs. $t^{-1/2}$ for $Cu(OH)_2$ NTs@GCE and c-MOFs@GCE; (D) The plot of I_{cat}/I_0 vs. $t^{1/2}$.

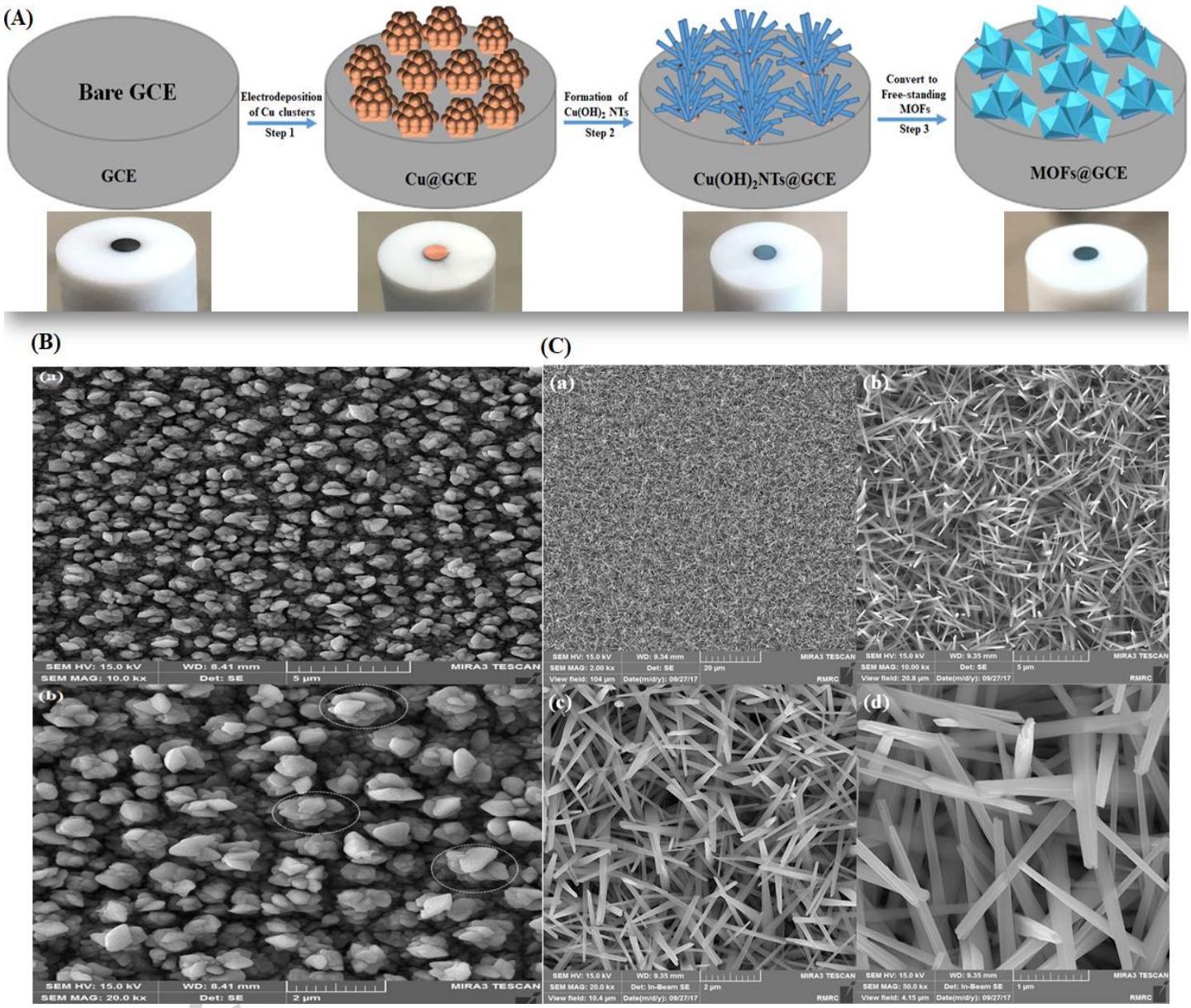
(A)
Bare GCE
GCE
Electrodeposition of Cu clusters
Step 1
Cu@GCE
Formation of Cu(OH)2 NTs
Step 2
Cu(OH)2NTs@GCE
Convert to Free-standing MOFs
Step 3
MOFs@GCE
(B)
(C)
(a)
(b)
(c)
(d)

Fig.1.

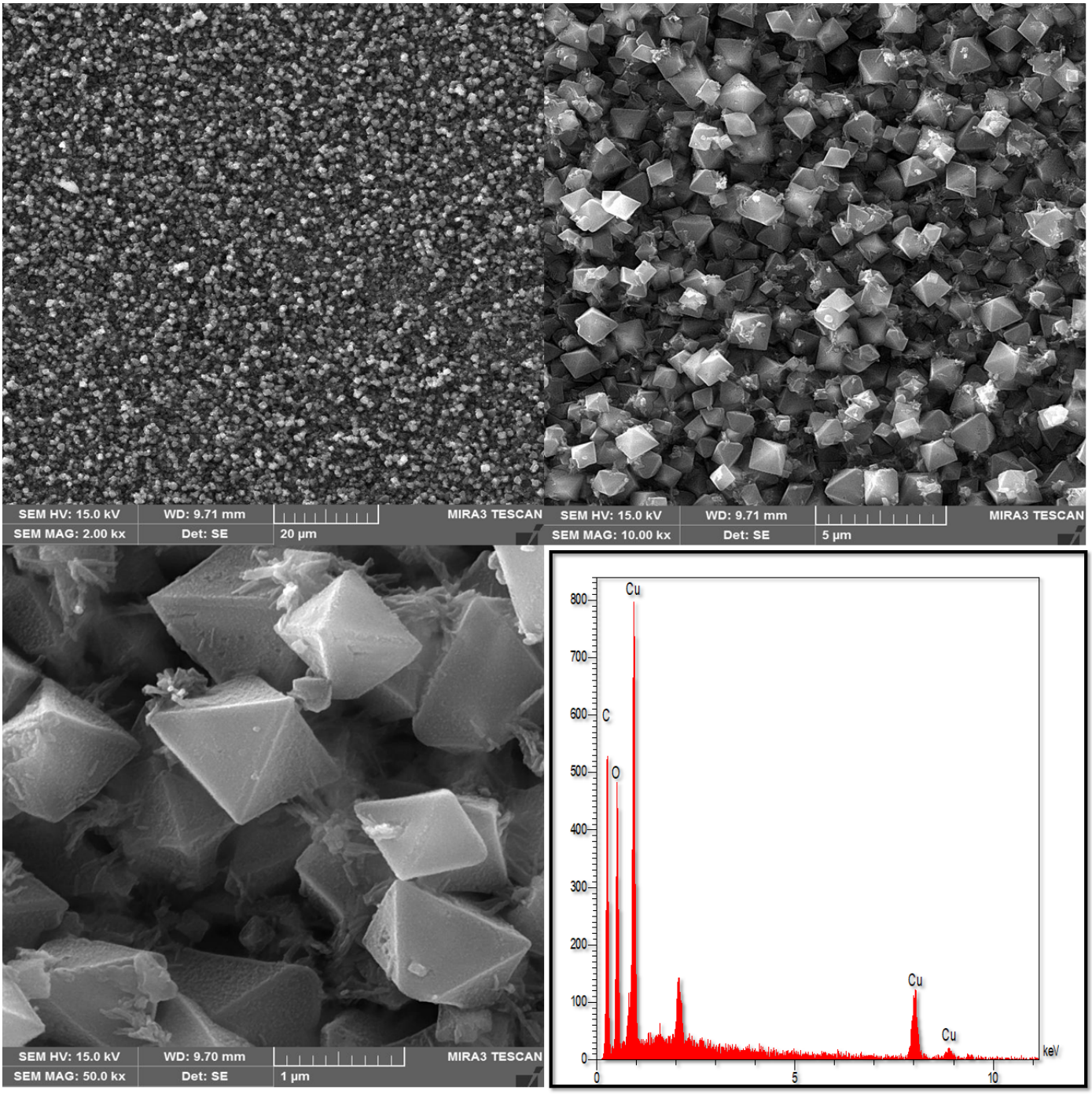
SEM HV: 15.0 kV
WD: 9.71 mm
MIRA3 TESCAN
SEM MAG: 2.00 kx
Det: SE
20 µm
SEM HV: 15.0 kV
WD: 9.71 mm
MIRA3 TESCAN
SEM MAG: 10.00 kx
Det: SE
5 µm
SEM HV: 15.0 kV
WD: 9.70 mm
MIRA3 TESCAN
SEM MAG: 50.0 kx
Det: SE
1 µm
Cu
C
O
Cu
Cu
800
700
600
500
400
300
200
100
0
0
5
10
keV

Fig. 2.

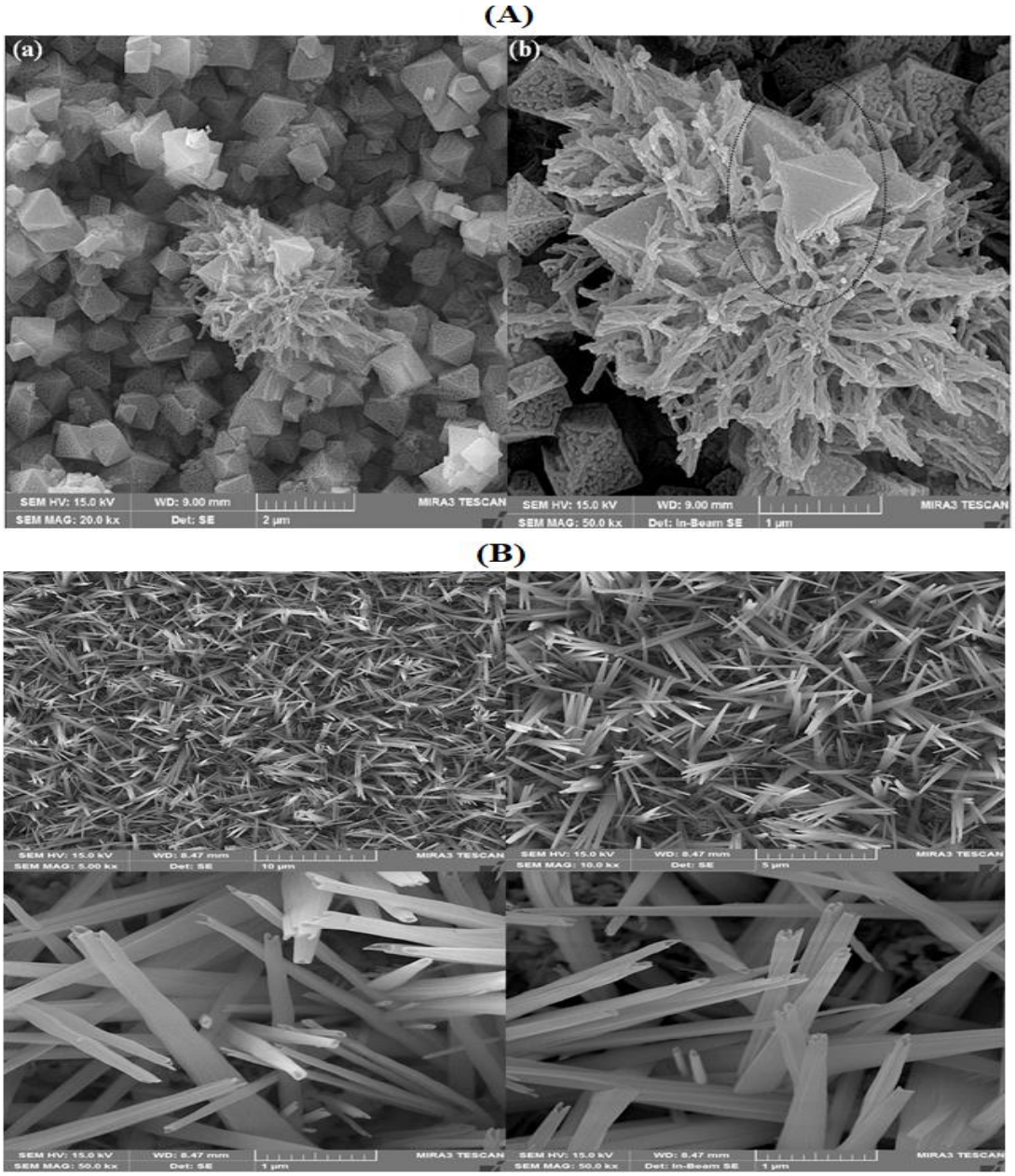
(A)
(a)
(b)
SEM HV: 15.0 kV
WD: 9.00 mm
MIRA3 TESCAN
SEM MAG: 20.0 kx
Det: SE
2 µm
SEM HV: 15.0 kV
WD: 9.00 mm
MIRA3 TESCAN
SEM MAG: 50.0 kx
Det: In-Beam SE
1 µm
(B)
SEM HV: 15.0 kV
WD: 8.47 mm
MIRA3 TESCAN
SEM MAG: 5.00 kx
Det: SE
10 µm
SEM HV: 15.0 kV
WD: 8.47 mm
MIRA3 TESCAN
SEM MAG: 10.0 kx
Det: SE
5 µm
SEM HV: 15.0 kV
WD: 8.47 mm
MIRA3 TESCAN
SEM MAG: 50.0 kx
Det: SE
1 µm
SEM HV: 15.0 kV
WD: 8.47 mm
MIRA3 TESCAN
SEM MAG: 50.0 kx
Det: In-Beam SE
1 µm

Fig. 3.

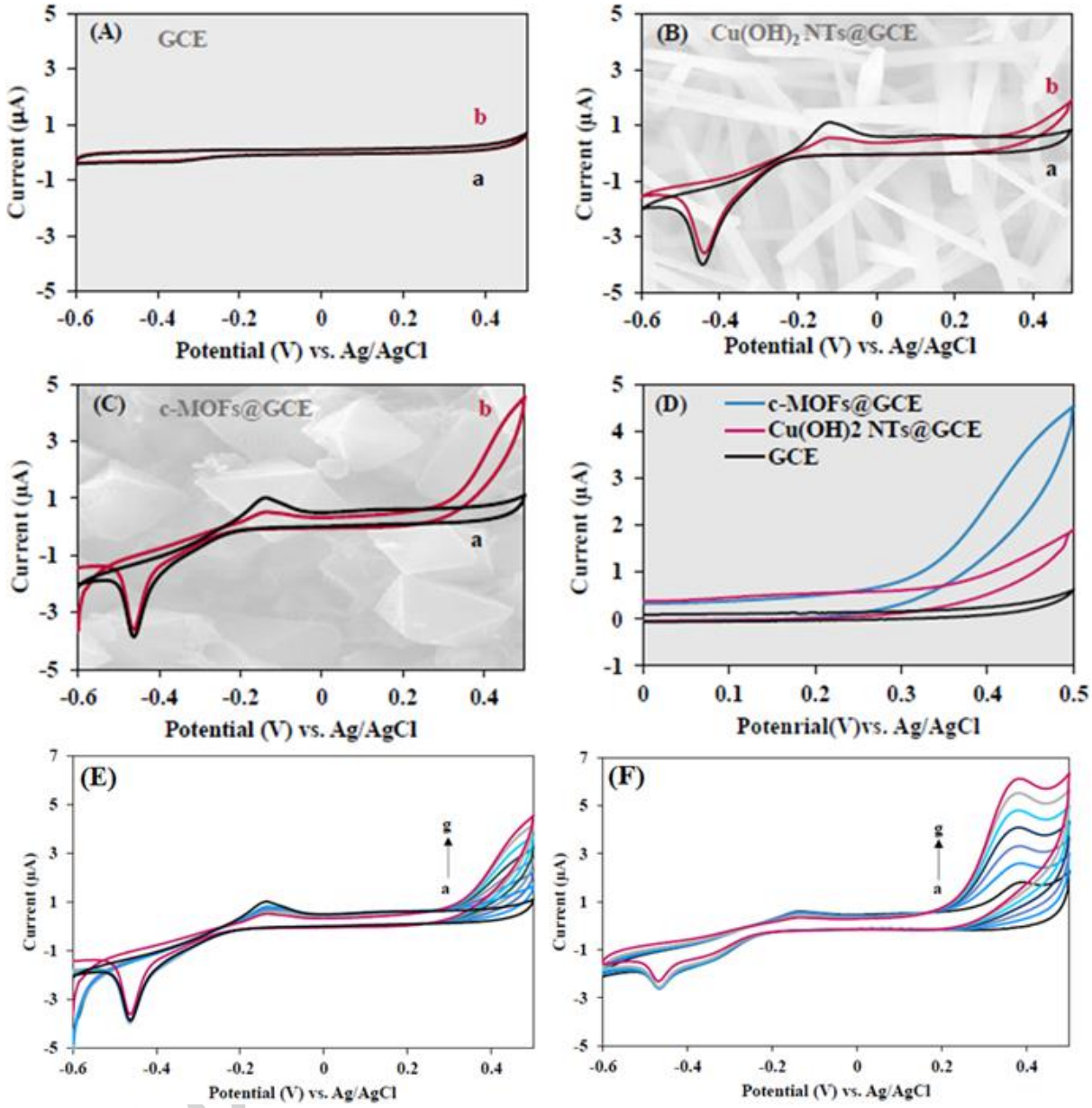
(A) GCE
b
a
Current (μA)
Potential (V) vs. Ag/AgCl
(B) Cu(OH)2 NTs@GCE
b
a
Current (μA)
Potential (V) vs. Ag/AgCl
(C) c-MOFs@GCE
b
a
Current (μA)
Potential (V) vs. Ag/AgCl
(D)
c-MOFs@GCE
Cu(OH)2 NTs@GCE
GCE
Current (μA)
Potenrial(V)vs. Ag/AgCl
(E)
g
a
Current (μA)
Potential (V) vs. Ag/AgCl
(F)
g
a
Current (μA)
Potential (V) vs. Ag/AgCl

Fig. 4.

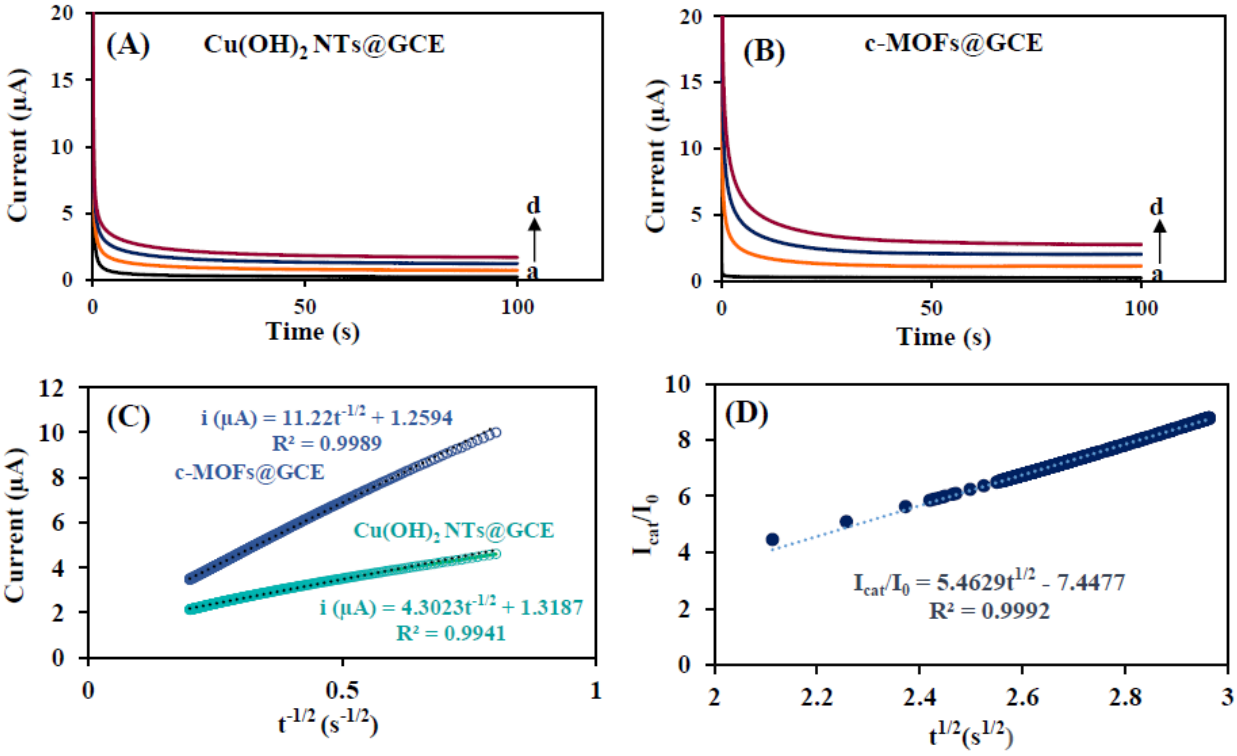

Fig. 5.

Highlights

- Rapid direct growth of MOFs on glassy carbon electrode (GCE) was developed.
- A novel free-standing MOFs electrode was fabricated based on this strategy.
- This rapid growth of MOFs was mediated by formation of vertically aligned Cu clusters and $Cu(OH)_2$ nanotubes arrays.
- This self-supported MOFs on GCE exhibited excellent analytical performances in non-enzymatic glucose sensing.